

NONLINEARLY CONSTRAINED MULTIPLE ELLIPSE FITTING

ALEXANDER M. GEURTZ
EPFL-DE-LTS, Ecublens
CH-1015 Lausanne, Switzerland

and

RICCARDO LEONARDI
Dept. of Electronics for Automation, University of Brescia
I - 25123 Brescia, Italy

and

MURAT KUNT
EPFL-DE-LTS, Ecublens
CH-1015 Lausanne, Switzerland

ABSTRACT

In this paper, a method is presented for estimating the parameters of a composite object consisting of several "primitive" objects that undergo rigid transformations. The objects are fitted to the features that are extracted from the data images. In order to simplify the problem, we restrict the analysis to the fitting of simple ellipses from two-dimensional contour data. The physical relations between the sub-objects are exploited as constraints on the solution space of the resulting optimization problem. An important feature of the method is that no attempt is made to establish closed-form relations. Instead, bounds on the parameters and on the constraints allow adapting the optimization to the uncertainty in the data and to the knowledge available *a priori*. The power of the method is that it can accommodate different primitive curves and constraints with the same general structure. The (admittedly, important) problem of segmenting the contour data set into disjunct sets is not treated in this paper. Application of the method is in the field of human motion estimation where each of part of the body is modelled by a separate geometric object. The method is illustrated with results on both artificially generated and real feature data.

1 Introduction

The work presented in this paper is performed in the context of a project on the analysis of human movement from image sequences. The body is modelled as a set of jointed objects that are considered representative for the overall shape and the task is to estimate the parameters of these objects from features detected in the image sequence. The objective of this paper is to report on the way we solved the problem of representing and estimating the relations between these objects from feature data.

One of the earliest approaches of applying image processing to the estimation of human body motion is due to O'Rourke and Badler¹. More recently physically based systems were introduced in the image processing world and applied to problems comparable to those stated above²⁻⁴. A large variety of parametric object models have been introduced over the last decades, ranging from simple rigid blocks to globally rigid generalized cylinders⁵ or quadrics with global and local deformations^{2-4,6-8}. Comparatively little attention has been paid to the problem of representing and estimating composite objects, i.e., objects consisting of two or more connected simple model objects. Due to the physical nature of the composite object, the parameters of the constituting primitive objects are not completely free, they are limited by certain relations.

The method presented in this paper differs from the above-cited literature in that no attempt is made to devise closed-form solutions. Instead, lower and upper bounds on the model parameters and on their constraining relations allow a smooth integration of the *a priori* knowledge that we have and the amount of uncertainty that has to be resolved. This enables a flexible structure where more complex models are formed from simple objects by simply adding the appropriate parameters and constraining relations, instead of having to solve a completely new problem.

The paper is organized as follows. After an initial section on the curve representation, the method is applied to the estimation of a single curve in Section 3. In Section 4 the method is applied to two articulated curves with known segmentation. Simulation results on artificially generated data illustrate the efficiency of the method. Results on real data relevant to the application are presented and discussed in a dedicated section, Section 5. Conclusions are drawn at the end of the paper. Current and future trends and developments are indicated as well.

2 Curve Representation

There are two main ways of representing curves and surfaces. Curves can be described either by an implicit relation between points \underline{x} on the curve and shape parameter vector \underline{p} such as $f(\underline{x}, \underline{p}) = 0$ or by an explicit relation between points \underline{x} on the curve, shape parameter vector \underline{p} , and driving parameter vector $\underline{\omega}$, such as $\underline{x} = g(\underline{p}, \underline{\omega})$. It is always possible, by reduction and elimination, to transform an explicit relation into an implicit one and vice-versa. Here, as we are performing an analysis rather than a synthesis, we prefer the implicit representation. The driving parameter allows an easy rendering for synthesis purposes, but in case of analysis a correspondence of the data with the driving parameter has to be established. This extra load favors the implicit representation, where the driving parameter is eliminated. The disadvantage of the implicit representation is the reduced sense of spatial distance. This will be discussed later.

For reasons of simplifying the analysis and without significant loss of generality, in the following the circle is considered as the basic implicit closed curve in two-dimensional space. This curve undergoes rigid transformations that will be called RST-transformations. The parameter vector \underline{p} contains the position, the orientation, and the sizes along the principal axes of the curve. Points \underline{x} on this ellipse are the RST-transformed points \underline{y} on the primitive circle:

$$\underline{x} = \mathbf{RS}\underline{y} + \underline{t} \quad (1)$$

with $\underline{y}^T \underline{y} - 1 = 0$ (the relation for the implicit circle), and where the rotation matrix \mathbf{R} and the scaling matrix \mathbf{S} are defined as

$$\mathbf{R} = \begin{bmatrix} \cos \theta & \sin \theta \\ -\sin \theta & \cos \theta \end{bmatrix} ; \quad \mathbf{S} = \begin{bmatrix} s_0 & 0 \\ 0 & s_1 \end{bmatrix} \quad (2)$$

The origin is displaced by a vector $\underline{t} = (t_0, t_1)^T$. The total implicit relation that is used here is obtained by eliminating \underline{y} from Eq. (1) using the relation for the implicit circle.

3 Single Curve Estimation

With the representation of the curve sufficiently simplified, attention is now turned to the estimation of the position, size, and orientation parameters of such a curve. In the following, four observations will be made: the necessity of estimating the parameters simultaneously, the importance of the choice of the error measure and of the optimization criterion, and the relevance of bounds on the parameters and the constraints.

The first observation is that it will be necessary to estimate all of the parameters simultaneously. Instead, in the classical approach to estimating ellipsoidal or in general superquadric shapes, first the center is derived from the centroid of the observations, then the main orientation from an eigenvector decomposition of the inertia matrix, and finally the size from some optimization procedure⁶. The disadvantage of this method is that errors in any stage of the process are propagated to the next, i.e., the result is biased. Furthermore, as it will be necessary to be able to put constraints on the admissible parameter values, we cannot allow to fix one or more of the parameters completely and then derive the others.

A second observation is the importance of the distance or error measure in the optimization procedure. Recent publications⁶⁻⁸ have addressed this issue, comparing the so-called In/Out error with radial and orthogonal distance measures. The In/Out error is the residual obtained by substituting observation $\underline{x} = \underline{x}_i$ for a given parameter vector \underline{p} in the implicit relation $f(\underline{x}, \underline{p})$. This does not constitute a Euclidean distance, but is fairly straightforward to calculate, and therefore attractive for a computationally rather intensive method as the one presented here.

A third observation considers the optimization criterion. Given a set of observations $\underline{x}_i, i = 1 \dots N$, the functional

$$J(\underline{p}) = \sum_{i=1}^N \rho(\|z_i\|) \quad (3)$$

is minimized, where z_i is the in/Out error

$$z_i = f(\underline{x}_i, \underline{p}) \quad (4)$$

given parameter vector \underline{p} . A quadratic measure is chosen for $\rho(\cdot)$, $\rho(y) = y^2$, in which case we obtain a least squares estimate.

A final observation is that it is often necessary to impose bounds on the admissible parameter values to avoid convergence to a physically non-plausible, but mathematically correct, minimum. This is due to the fact that the error measure does not put a penalty

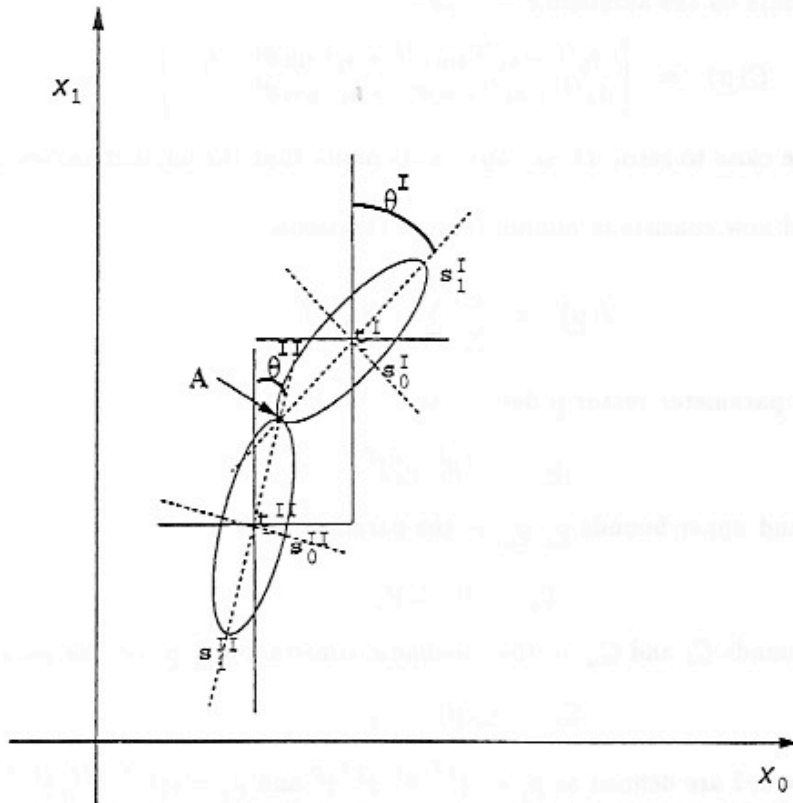


Figure 1: Composite curve configuration.

on the curve being incomplete. Simple bounds would be to impose that the center is somewhere within the swarm of points \underline{x}_i , and that the size parameters range from a minimum to a maximum value. This is equivalent to putting a bounding box or convex hull around the data.

At this point, the curve fitting method consists in minimizing the criterion in Eq. (3), subject to bounds on the parameter vector \underline{p} , given a set of observations \underline{x}_i , and where the errors-of-fit z_i are nonlinear functions of observations and parameters.

4 Composite Curve Estimation

Now consider the case of fitting two curves to the data with additional constraints describing the relations between the parameter vectors of the curves. These additional constraints are often imposed because of physical limitations to the problem. The problem of how to obtain two distinct point sets related to the curves, the *segmentation* problem, is treated in another paper⁹, here the segmentation is supposed to be known. The constraints imposed depend on the configuration of the composite model object. Given our intended application, the additional constraint imposed here is that the endpoints touch. Referring to Figure 1 (freely redrawn from Hemami and Chen¹⁰), this would mean that the following

nonlinear constraints on the admissible solutions:

$$\underline{C}(\underline{p}) = \begin{bmatrix} t_0^{II} + s_1^{II} \sin \theta^{II} + s_1^I \sin \theta^I - t_0^I \\ t_1^{II} + s_1^{II} \cos \theta^{II} + s_1^I \cos \theta^I - t_1^I \end{bmatrix} \quad (5)$$

are bounded to be close to zero. These constraints imply that the implicit curves meet in point A.

The method now consists in minimizing the functional

$$J(\underline{p}) = \sum_{j=1}^2 \sum_{i=1}^{N_j} \rho(\|z_{ij}\|) \quad (6)$$

for the composite parameter vector \underline{p} defined as

$$\underline{p} = (\underline{p}_1^T, \underline{p}_2^T)^T \quad (7)$$

subject to lower and upper bounds $\underline{p}_l, \underline{p}_u$ on the parameters

$$\underline{p}_l \leq \underline{p} \leq \underline{p}_u \quad (8)$$

and subject to (bounds \underline{C}_l and \underline{C}_u on the) nonlinear constraints $\underline{C}(\underline{p})$ on the parameters

$$\underline{C}_l \leq \underline{C}(\underline{p}) \leq \underline{C}_u \quad (9)$$

The vectors $\underline{p}_i, i = 1, 2$ are defined as $\underline{p}_1 = (\underline{t}^{I}, \theta^I, \underline{s}^{I})^T$ and $\underline{p}_2 = (\underline{t}^{II}, \theta^{II}, \underline{s}^{II})^T$. By definition, unspecified bounds are at minus (lower bound) or plus (upper bound) infinity.

At this time it is useful to elaborate the role of bounds and constraints. Bounds are defined here as lower or upper limits on the admissible values of the parameters or the constraints. The constraints (or more correctly, constraint equations) express linear or nonlinear relations between parameters. The constraint equations are derived from physical relations and describe the spatial structure of the composite object. The bounds are determined either by physical constraints (e.g., sizes are positive) or by uncertainty considerations (e.g., given a previous estimate an uncertainty interval of $\pm 25\%$ with respect to this previous estimate seems reasonable.) In practice both sources of bounds are used. If, as an example, the sizes of the two curves along the vertical object axes are supposed to be equal (physical constraint), the corresponding constraint equation would be $c(\underline{p}) = s_1^I - s_1^{II}$. Now the lower and upper bounds on this constraint determine how much this constraint has to be enforced. For example, if we want these sizes to be at most 0.5 measurement unit apart, the lower and upper bounds of the corresponding constraint equation would be set at -0.5 and 0.5 , respectively. If there is little *a priori* knowledge on the values of the parameters or the quality of the data, these bounds can (and must) be taken quite wide.

This representation of bounded constraint equations adds the necessary flexibility that the closed-form solutions lack. Moreover, adding or deleting constraints is very simple.

The nonlinearly constrained optimization problem stated above is not a trivial one. The algorithm applied in this paper is described in detail in the excellent documentation provided with the NAG software library¹¹. In resume, a sequential quadratic programming (SQP) algorithm is applied to the problem, with search directions derived from a quadratic

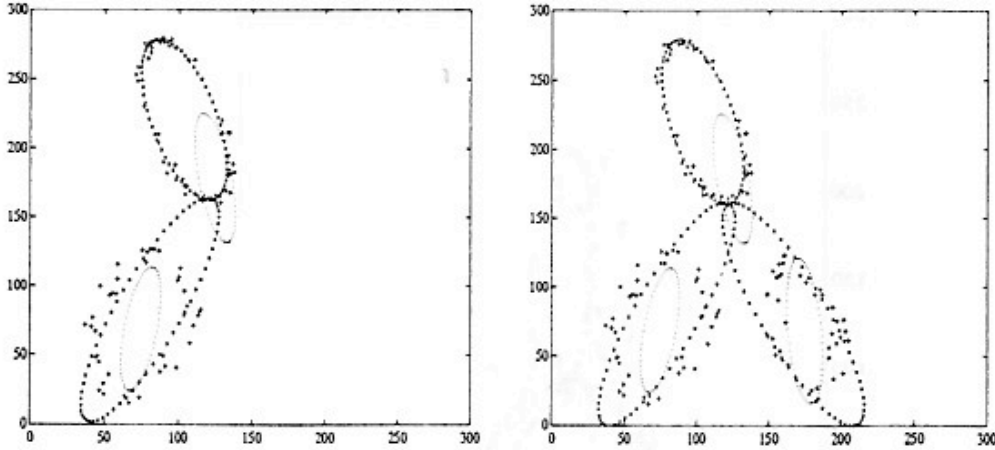


Figure 2: Point sets and constrained fitting results.

programming algorithm. Bounds on parameters and constraints are treated separately. The SQP algorithm leads to an iterative sequence $\underline{\mathbf{p}}^{(k)}$ with an update $\alpha^{(k+1|k)}\underline{\mathbf{p}}^{(k+1|k)}$ where $\alpha^{(k+1|k)}$ is the steplength and $\underline{\mathbf{p}}^{(k+1|k)}$ is the search direction. This sequence tends, under certain conditions, to a solution $\underline{\mathbf{p}}^*$ of the problem, given by the “first-order Kuhn-Tucker point.”

5 Results

In this section, the method is illustrated with some results obtained with artificially generated contour points and with contour points obtained from sampling contours extracted from a real image.

First, in Figure 2, results on artificially generated feature points are shown. In the leftmost plot of this figure, two distinct point sets are plotted, indicated with the + - signs. The location error (jitter) is higher for the points belonging to the lower curve than for those belonging to the upper one. Note that the curves are quite far apart, in order to better see the effect of the nonlinear constraint. The initial estimates for the two curves are drawn with dotted lines and the stars indicate the final result obtained. The nonlinear “touching” constraint was set to quite tight (± 0.5). This bound means that the two endpoints of the two curves are allowed to be at a distance of half a unit distance (pixel), or about 1 percent. Bounds on the size parameters were set at $\pm 50\%$ of the initial values. In real situations these bounds should of course be derived from an analysis of the data, which is still a research issue. Here, we only wish to illustrate the feasibility of the method. In the rightmost plot of the same figure, a three-body structure is estimated from three distinct point sets. For each of the three two-body relations, two relations such as in Eq. (5) are added to the total constraint vector $\underline{\mathcal{C}}(\underline{\mathbf{p}})$. The final result is again indicated with the stars. It can be concluded from the results shown in Figure 2 that, despite the large gap and the considerable noise, the constrained fitting yields quite

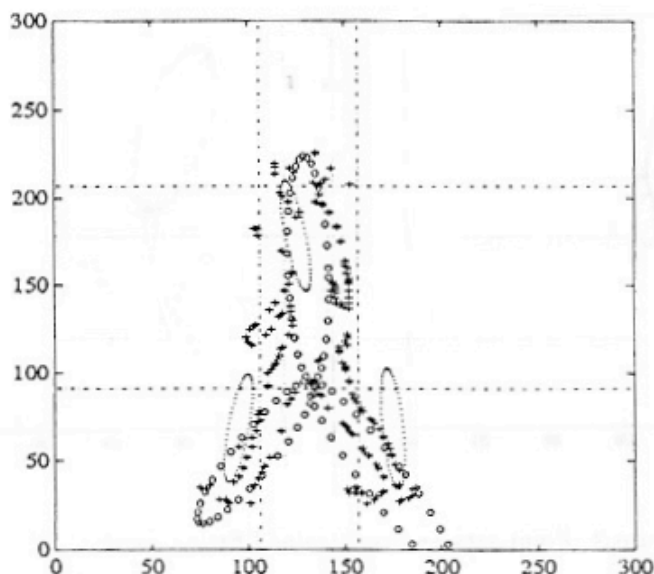


Figure 3: Simultaneous constrained segmentation and fitting of point sets.

satisfactory results, although difficult to evaluate and analyze.

Second, in Figure 3, the results obtained from fitting the constrained three-body model to real contour points are shown. These points were randomly sampled along the contours extracted from an image of a person walking. The contours points are plotted with the $+$ -signs, the initial estimates with the dotted curves. The final results is plotted with the o -signs. The result is obtained here using the simultaneous segmentation and estimation algorithm described in a companion paper⁹. The nonlinear constraints have been perfectly satisfied.

6 Conclusions

We have presented a new method for estimating the parameters of composite curves. The curves are represented by implicit relations and the physical limitations between the objects that constitute the global structure are expressed as nonlinear constraints on the solution space of the resulting optimization problem.

The most important feature of the algorithm is that no attempt is made to establish closed-form solutions to the problem. Instead, lower and upper bounds on the constraints and on the parameters allow to loosen the constraints if the uncertainty in the data necessitates so. This also partly overcomes modelling errors very much in the way noise is added to a Kalman filter in order to give it more stability.

We are currently working on a hierarchical way of propagating from a simple curve representation to a composite one, the parameter values, the membership coefficients, and

the bounds on the linear and nonlinear constraints and on the parameters. This reduces the problem of being trapped in one of the numerous local minima of the error functional and also the computational complexity of the method.

Other issues of interest include: a more rigorous way of relating uncertainty in the data to the values of the bounds on the parameters and the constraints (a "constrained covariance"), the extension to sequences, and finally using a more robust error functional would be desirable. With this powerful tool, many disturbing outliers could be effectively removed.

References

1. J. O'Rourke and N.I. Badler. Model-based image analysis of human motion using constraint propagation. *IEEE Trans. Pattern Analysis and Machine Intelligence*, 2(6):522-536, November 1980.
2. D. Terzopoulos and D. Metaxas. Dynamic 3D models with local and global deformations: Deformable superquadrics. *IEEE Trans. Pattern Analysis and Machine Intelligence*, 13(7):703-714, 1991.
3. A. Pentland and B. Horowitz. Recovery of nonrigid motion and structure. *IEEE Trans. Pattern Analysis and Machine Intelligence*, 13(7):730-742, 1991.
4. A. Pentland and S. Sclaroff. Closed-form solutions for physically based shape modelling and recognition. *IEEE Trans. Pattern Analysis and Machine Intelligence*, 13(7):715-729, 1991.
5. J. Ponce, D. Chelberg, and W.B. Mann. Invariant properties of straight homogeneous generalized cylinders and their contours. *IEEE Trans. Pattern Analysis and Machine Intelligence*, 11(9):951-966, September 1989.
6. F. Solina and R. Bajcsy. Recovery of parametric models from range images: The case for superquadrics with global deformations. *IEEE Trans. Pattern Analysis and Machine Intelligence*, 12(2):131-147, February 1990.
7. Alok Gupta, Luca Bogoni, and Ruzena Bajcsy. Quantitative and qualitative measures for the evaluation of the superquadric models. In *Proc. Workshop on Interpretation of 3-D Scenes*, pages 162-169, Austin, TX, USA, Nov 27-29 1989.
8. A.D. Gross and T.E. Boult. Error of fit measures for recovering parametric solids. In *Proc. Second Int. Conf. on Computer Vision*, pages 690-694, Tampa, FL, USA, Dec 5-8 1988.
9. Alexander M. Geurtz, Riccardo Leonardi, and Murat Kunt. Fuzzy segmentation of multiple articulated elliptical curves from sparse contour data. In H. Dedieu, editor, *European Conference on Circuit Theory and Design*, Davos, Switzerland, 31 Aug - 3 Sept 1993.
10. Hooshang Hemami and Ben-Ren Chen. Stability analysis and input design of a two-link planar biped. *Int. J. of Robotics Research*, 3(2):93-100, Summer 1984.
11. Numerical Algorithms Group. *NAG Fortran Library Documentation, Release 15*. NAG Ltd, Oxford, UK, 1991.